Acoustic Dampening of Propellers

CJ "Nehemiah" Jordan[1], Hayden Pendarvis[2], Bartlet Pollock[3], Nate Wylie[4]
Mississippi State University, Mississippi State, MS 39762

Throughout history, powered flights have been plagued by high noise levels. With the increase in the use of propeller-driven aircraft near highly populated areas and recent advancements in electric-powered flight, noise mitigating design considerations will need to be implemented, to alleviate the noise production of electric-powered aircraft. Research is considered, and an analysis is performed to study aerodynamic performance of an aircraft propeller. Ansys Student CFD software is used to simulate a single propeller, with a variety of modifications to the trailing edge of the propeller blades. Once the CFD programs are validated, study of acoustic dampening techniques leads to implementing trailing edge serrations to the propeller in three different approaches. This leads the team to assess the overall performance of the four total propeller geometries, and how the results can change propeller design considerations in the future.

I. Introduction

Most people would agree that one common problem has seemingly plagued powered flight from the very beginning; all aircraft produce noise levels much higher than would be preferred. In fact, as modern air travel has become more prevalent, the Federal Aviation Administration (FAA) has placed progressively tighter restrictions on the noise levels produced by aircraft. In addition, growing population and strain on space has even increased societal interest in air transportation within cities. However, current aircraft configurations would create an unnecessary amount of noise pollution, leading to research on how aircraft can be designed to produce less noise in the future. Currently, engineers are hard at work, devising ways to make electric flight possible, meaning the quintessential droning of an aircraft overhead may soon become a thing of the past. This leaves many aircraft with one major source of noise: the propeller. Therefore, the team aims to focus solely on ways in which propellers can be designed to perform exceptionally, while producing less noise than their predecessors.

II. Procedure

To begin investigating the issue at hand, research began on several methods of mitigating the acoustic signature of propellers, both successful and unsuccessful. It was found that serrating the trailing edge of a propeller blade significantly reduces its noise signature. Additionally, it was found that applying backward sweep to the outer portion of the propeller blades helps reduce acoustic pressure levels that result from the extreme speeds of the propeller blades at their tips. This is mainly due to reducing the intensity of the shock that is produced by the outer region of the blades. Since the outermost region of the blade is closest to transonic/supersonic flow, it is best to apply progressive sweep to blades that will operate at revolution per minute (rpm) ratings that will result in transonic or supersonic flow. Extending this train of thought, applying super critical airfoil shape at the ends of propeller blades should reduce noise by first reducing shock intensity, as well. Moving on from initial research, familiarity with the Ansys software was increased by utilizing a free tutorial for simulating a rotating propeller

[1] ASE Undergraduate Student, Mississippi State University, 1899 Whitehawk Court, Student
[2] ASE Undergraduate Student, Mississippi State University, 375 College View Street, Student
[3] ASE Undergraduate Student, Mississippi State University, Student
[4] ASE Undergraduate Student, Misssissipi State University, Student

To begin, a geometry module is created on the Ansys Workbench and a publicly available CAD file of an APC 16x8E propeller, as seen in Figure 1, is imported into said module. Initially, the propeller was found to be oriented off-center, with respect to the geometric origin. This complicates the set-up portion of the experiment when an axis of rotation needs to be assigned, in terms of the x, y, and z axes. To correct the misalignment, the geometry is edited in SpaceClaim. Upon entering SpaceClaim, the generate button may need to be selected in order to make the geometry of the previous module visible. This principle holds for each module in Ansys. Moving on, the propeller can be accurately centered by utilizing the Move tool. This tool allows the user to translate the propeller along the three axes, and simultaneously illustrates the displacement between the propeller's geometric center, and the origin. To center the propeller on the universal origin, select the Move tool and then box the entire propeller by clicking and drawing a box around it. An origin that coincides with the geometric center of the propeller will appear. Select the 'Up To' tool on the side panel of the Move tool options. Now the universal origin can be selected, which will automatically snap the propeller center to the universal origin. The propeller is now centered. Now, SpaceClaim can be exited. The rest of the geometry definitions will be made in Design Modeler. Once Design Modeler is opened and the geometry has become visible, two separate cylindrical shapes will need to be created. The first shape needs to be drawn close in size to the propeller, with the propeller centered in the resulting region. This small region will later serve as the domain that rotates at the assigned rpm value, with respect to the static domain. Once completed, repeat the sketch process for a larger region; this will be the static region. Each of these two regions need to be defined as Add Frozen operations. As a rule of thumb, sizing the static region to be around 10 times the size of the propeller should allow the user to avoid flow interference from the walls. Lastly, two subtracting Booleans are created. The first Boolean assigns the propeller as the tool body and the rotating domain as the target body. For the second Boolean, the rotating domain is selected as the tool body and the static domain as the target body. Figure 2 can be used to verify end resultant geometry.

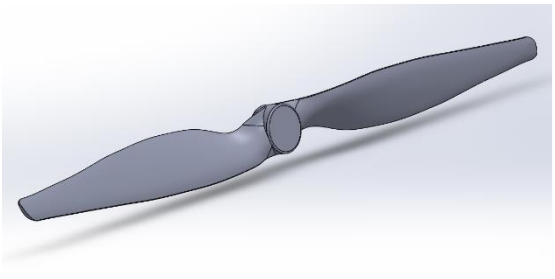

Figure 1: APC 16x8E Propeller

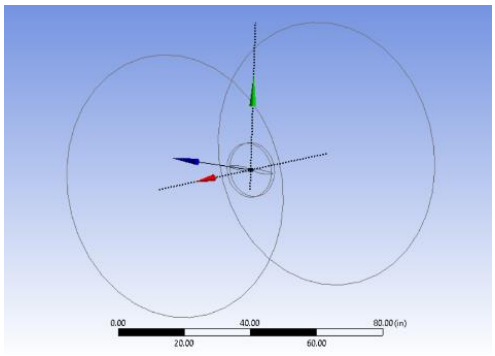

Figure 2: Completed Geometry

Once the geometry is completed and closed, a Fluid Flow (Fluent) project is created, which is placed such that the previously created geometry will be fed into the rest of the project. When dragging the Fluid Flow (Fluent) project over to the schematic window, hover the mouse above the arrow at the bottom right corner of the Geometry module. This tells the system to feed the geometry to the Fluid Flow (Fluent) project. Figure 3 shows the resulting block diagram. Moving forward, the Mesh module is selected and updated before being opened. Upon opening Mesh, element size, min size, and maximum tetrahedral size can be manipulated in order to gain a satisfactory mesh. Also, if there are particular regions of interest, right-click on Mesh, select sizing and the user ahs the ability to assign specific mesh sizing to particular regions in terms of faces, bodies, and spherical proximities. This can be very useful in the instance of utilizing large geometric domains that don't necessarily need full mesh resolution throughout. For instance, the main focus of this experiment is in analyzing pressures and flows on and very close to the surface of the propeller. Therefore, the sizing tool may be using to increase mesh fineness at the propeller, while allowing the static domain to remain relatively coarse.

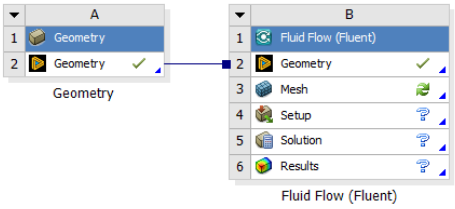

Figure 3: Complete Block Diagram

After closing the Mesh module and updating the Setup Module, Setup is opened. A prompt appears before the module completely opens. Double precision needs to be selected, as well as setting the solution process parameters to four parallel solution processes. In the General panel, the system is set to a Pressure-Based solver, Transient time, and define gravity to be -9.81 meters per second (m/s) in the y-direction. Next, the Viscous Models tab is selected, and the k-epsilon (2 eqn.) model is chosen. The model is set to be Realizable and to use Scalable Wall Functions, before clicking okay. Next, in Cell Zone Conditions, Mesh Motion is selected, and the axis of rotation is defined to be the x-direction. This is determined solely by the orientation of the propeller. The rpm value for the propeller can also be set in this window. For this experiment, this value remained constant at 5000 rpm. Additionally, units can be set in the units' tab, which is found at the top left of the page. The units being used for this experiment were rev/min for angular velocity, and pounds force (lbf) for thrust force. Moving on, Initialization is selected, and Hybrid Initialization is selected. The system needs to be initialized before each run, if any settings have been changed since the preceding run. This will serve as the last step before moving to Run Calculation in the future. Once this is done, the user can manipulate the number of time steps, number of iterations per time step, and time step size. Some trial and error may be necessary to ensure valuable data. For instance, the system can complete the iterations without arriving at a sufficient solution. Therefore, the analysis may need to be run at several different values of iterations, while keeping all other settings constant. Once the solution stops showing signs of inconsistency, these settings should be maintained for further calculation. Once all settings are determined, Select Run Calculation.

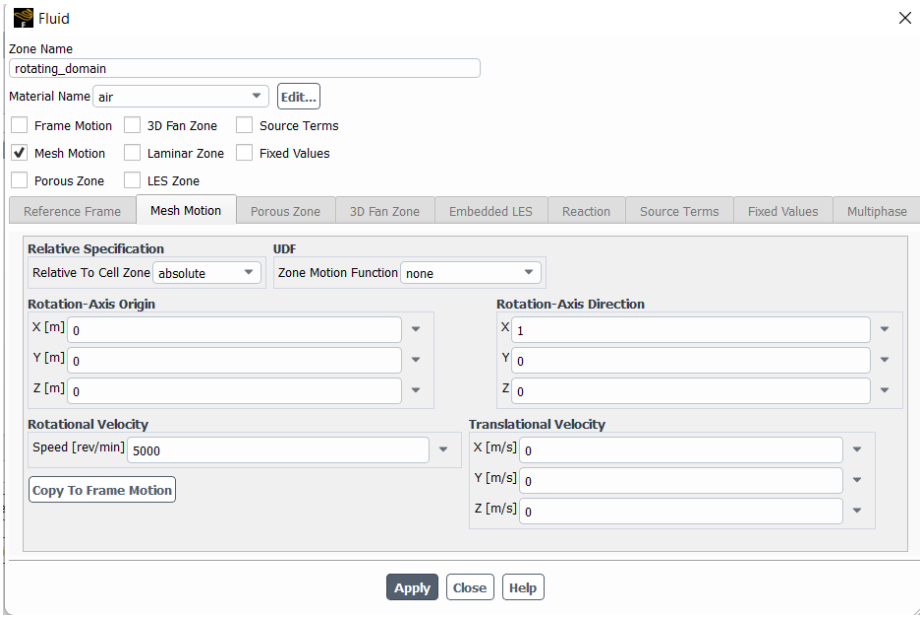

Figure 4: Cell Zone Condtiions

In order to find the thrust force from the analysis, Forces was selected after entering the Reports tab. This will allow the user to generate a thrust force report after each run. The system will print force values for each axis. The force value that correlates to the propeller axis of rotation is the calculated thrust value. Figure 5 shows the data gathered from running the analysis at 100 time steps for 10 iterations per time step. The time step was set to 0.015s. These parameters were gathered by the team as a result of performing a validity study. In order to validate the aerodynamic analysis program, the team began performing consecutive runs at increasingly smaller element sizing, with respect to the mesh. By doing this, the team was able to create a program that consistently converges to acceptable values within a consistent range of interations. The team ws eventually able to plot data CFD solution values against the APC data and validate successful function of the aerodynamic CFD program. Figure 1 illustrates the data used to validate the function of the aerodynamic CFD program. From here, the same procedure will be undergone for the acoustic CFD program, ensuring accurate function of the calculations for future use.

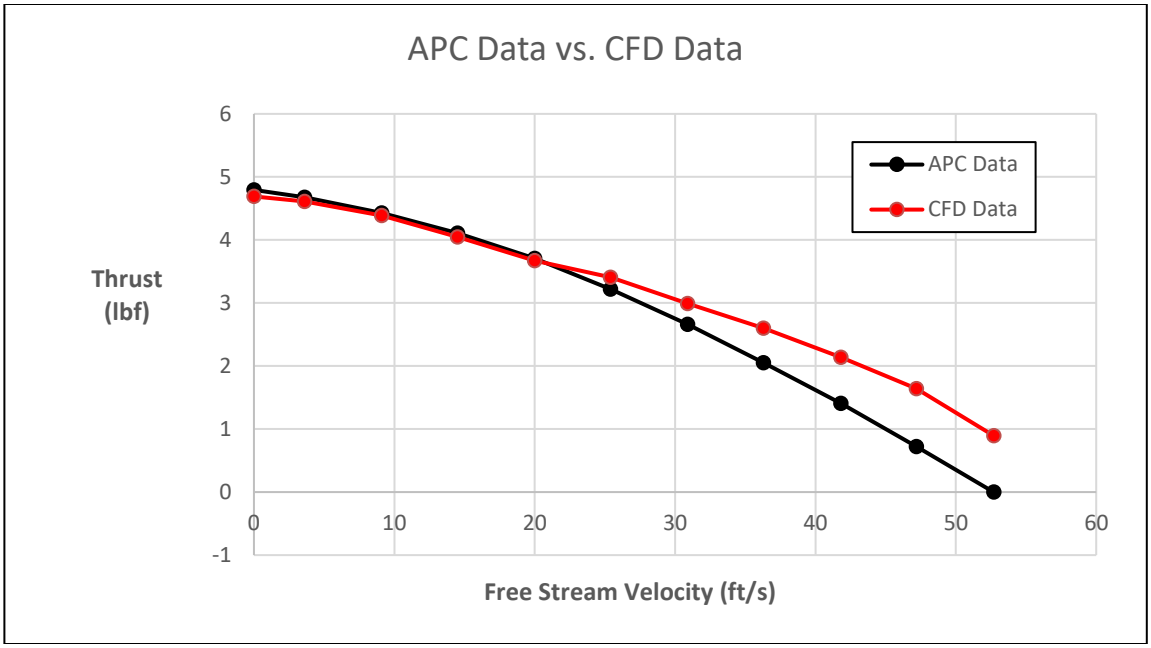

Figure 5: Aerodynamic CFD Validation

III. Results

The team is currently in the process of debugging and validating the CFD programs that will be used to perform the proposed study. Once validations are completed, the team will select a base propeller model and apply trailing-edge serrations to the full length, inner third, and outer third of the propeller's blades for comparison. Performing this experiment will yield data that allows the team to judge where exactly trailing edge serrations, as well as other methods, are most beneficial to be implemented onto propeller designs. Additionally, these programs will be made available to the Mississippi State University Aerospace Engineering Department, allowing future students to perform further studies on propeller design.

IV. Conclusion

The validation of both the aerodynamic and acoustic simulations is currently underway and scheduled to be completed within the following week. As for the data to be gathered, the team hypothesizes that trailing edge serrations may be most beneficial when implemented close to the blade tips, as opposed to being closer to the base of the propeller. This idea stems from the fact that the nature of propellers results in significantly increased relative flow velocities, as the observer moves toward the tips of the propeller blades. This is likely to contribute to the majority of the aeroacoustic signature of the propeller. Therefore, modifications like trailing edge serrations may be best focused at the outer regions of the propeller blades.

References

[1] *A study on Propeller & Rotor Noise and Reduction of their Acoustic Intensity*. Boulanger, Neils. https://spaceandscience.fr/en/blog/helicopter-noise-study

[2]Analysis Systems (ANSYS) Student CFD Software. 2022. https://www.ansys.com/academic/students

[3]*Ansys Fluent: Simulation of a Rotating Propeller.* Ansys How To. Published online 14 March, 2018. https://www.youtube.com/watch?v=iAm2f7AHLfg&t=61s

[4] *Ansys Fluent Simulation of a Rotating Propeller.* Ansys How To. Published online 14, March, 2018. https://www.youtube.com/watch?v=iAm2f7AHLfg&t=61s

[5]*CFD on Propeller Fan with Acoustic.* CAD CAE CFD. Published online 19 August, 2022.

[6]*Noise Reduction Potential of Swept Propeller Blades*. Drobietz, Dr. R, et al. CEAS Forum on Aeroacoustics of Rotors and Propellers, 9 June 1999, pp. 65–77.

[7] *How to Calculate Thrust Force on a Rotating Propeller Blade Using CFD ANSYS(Fluent) 19.1 || Part 1*. Published online 13 April, 2019. Alves, Arjen. https://www.youtube.com/watch?v=sHTSyWL_gds&t=214s

[8] *How to Calculate Thrust Force on a Rotating Propeller Blade Using CFD ANSYS(Fluent) 19.1 || Part 2*. Published online 13 April, 2019. Alves, Arjen. https://www.youtube.com/watch?v=9xnubvVsvyM&t=12

[9] *Propeller Noise Reduction by Means of Unsymmetric Propeller Spacing*. Dobrzynski, W. Published online Volume 163, Issue 1. 8 May, 1993. Pages 123-126. https://www.sciencedirect.com/scicence/article/pii/S0022460X83711521?via%3Dihub

[10]*Research of Noise in the Unmanned Aerial Vehicle's Propeller using CFD*. Vijayanandh R, Ramesh M, Raj Kunmar G, Thianesh UK, Venkatesan K, Senthil Kumar M. August 2019. https://www.ijeat.org/wp-content/uploads/papers/v8i6S/F10310886S19.pdf

[11] "*Status of Research on Propeller Noise and Its Reduction*." *The Journal of the Acoustical Society of America*, Regier, Arthur A., and Harvey H. Hubbard. vol. 25, no. 3, 1953, pp. 395–404., https://doi.org/10.1121/1.1907054.